JOURNAL OF AIRCRAFT
Vol. 43, No. 5, September–October 2006

Engineering Notes

ENGINEERING NOTES are short manuscripts describing new developments or important results of a preliminary nature. These Notes should not exceed 2500 words (where a figure or table counts as 200 words). Following informal review by the Editors, they may be published within a few months of the date of receipt. Style requirements are the same as for regular contributions (see inside back cover).

Experimental Investigation on Forced Boundary-Layer Transition of Axisymmetric Inlet and Numerical Verification

Fan Xiao-qiang,* Li Hua,† Jia Di,‡ and Yi Shi-he§
National University of Defense Technology, ChangSha, 410073, China

DOI: 10.2514/1.17040

Nomenclature

cal	=	calculational results using CFD method
exp	=	experimental results
k-epsilon	=	CFD results using *k*-epsilon turbulence model
No trip	=	experimental results of laminar boundary-layer case
With trip	=	experimental results of turbulent (or transitional) boundary-layer case
x	=	axial position along the generatrix of the inlet center cone

Introduction

HYPERSONIC inlet is an important component of the air-breathing hypersonic vehicle [1]. A large amount of experiments have been performed to improve the inlet performance or develop the inlet design method. However, in most wind tunnel tests, being restricted by the test condition of these ground facilities, some flow parameters are different from those in actual flight [2]. So, how to analyze, evaluate, and use the experimental data for inlet design is a primary problem to be solved. The most important difference between the actual flight and the ground test is the diversity of the boundary-layer states. In most hypersonic wind tunnels [3,4], the flow Reynolds number is smaller than that in actual flight; the boundary layer may remain laminar all along the inlet walls, despite the turbulence intensity of the coming freestream flow which might be larger than that in actual flight. However, in hypersonic actual flight, a natural boundary-layer transition may exist on the forebody because of a relatively large length scale and Reynolds number. The influence caused by different boundary-layer states should be taken into account in experimental data analysis, to use the present inlet experimental database or guide future experiment research.

The starting characteristics of the inlet are an important factor in inlet performance evaluation. Two types of unstart behavior have been classified as "hard" or "soft" by Van Wie in [5]. The hard unstart is mainly caused by overcontracting, whereas the soft unstart is mainly caused by viscous or separation. Many papers about inlet start performance were published in recent years. One of these results indicates that the starting limit is mainly restricted by the inner contractive ratio CR_{in} and hard unstart will not occur if the CR_{in} is not excessively large. On the other hand, the soft unstart occurs frequently in some inlets for shocks generated by the cowl or side wall may cause a relatively large separation in the inlet, and the shocks cannot be dispelled completely in many cases nevertheless. So, one of the most important works is to design an appropriate inlet configuration to reduce separation. Some typical technical efforts such as the swept cowl lip, the swept side wall leading edge [6], the stepped strut [7], the convex throat shape [8], and the boundary-layer bleed [9] were adopted and researched to reduce separation and improve inlet performance, and all of these technical means were proved to be useful. As we know, the separation region will become smaller if the boundary layer is transited to turbulence. The forced boundary-layer transition may be another useful method to reduce the separation and may facilitate the inlet start.

The total pressure recovery capability is another important factor in the inlet performance evaluation, so that reducing the separation cannot only avoid inlet soft unstart, but also improve the inlet total pressure recovery.

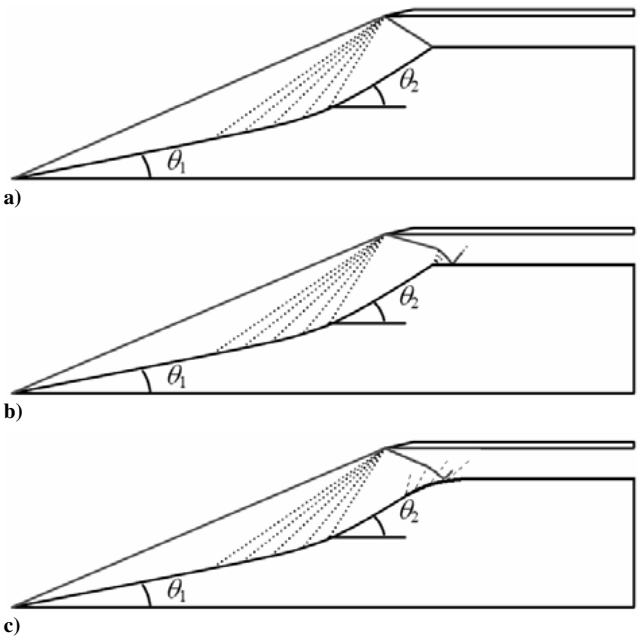

Fig. 1 Sketch of flow structure in the inlet.

Presented as Paper 3551 at the 41st AIAA/ASME/SAE/ASEE Joint Propulsion Conference & Exhibit, Tucson Arizona, 10–13 July 2005; received 5 June 2005; revision received 23 October 2005; accepted for publication 24 December 2005.

*Ph.D. Candidate, Institute of Aerospace and Material Engineering; xiaoqiangfan@hotmail.com.

†Professor and Director of Hypersonic Vehicle Design Research in Aerospace Engineering Project, Institute of Aerospace and Material Engineering.

‡Ph.D. Candidate, Institute of Aerospace and Material Engineering.

§Professor of Hypersonic Experimental Research in Aerospace Engineering Project, Institute of Aerospace and Material Engineering.

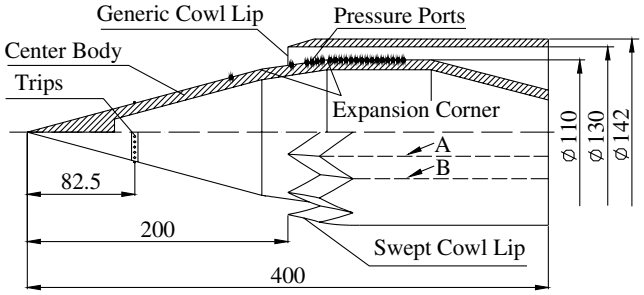

Fig. 2 Experimental model.

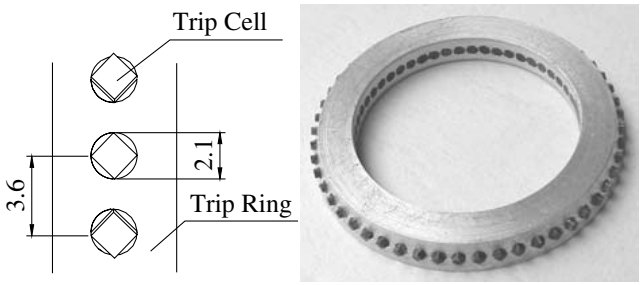

Fig. 3 Boundary-layer transition device.

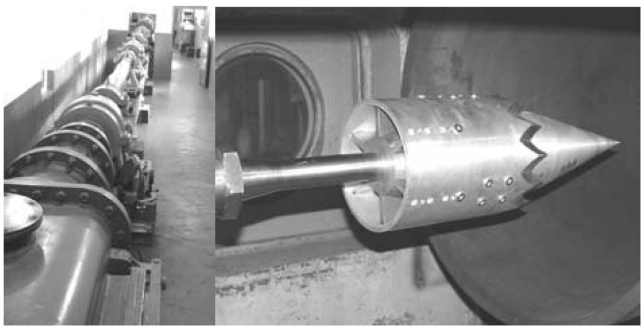

Fig. 4 KD-01 gun tunnel and the inlet model.

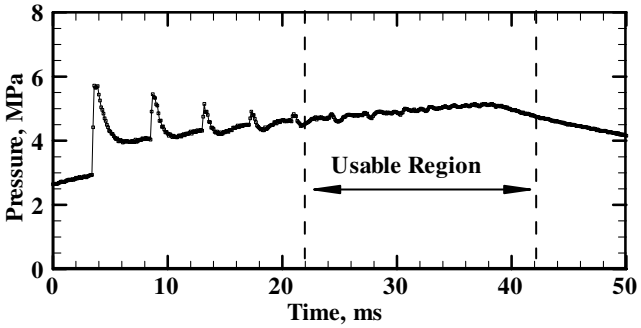

Fig. 5 Pressure signal acquired from the low-pressure part of the wind tunnel.

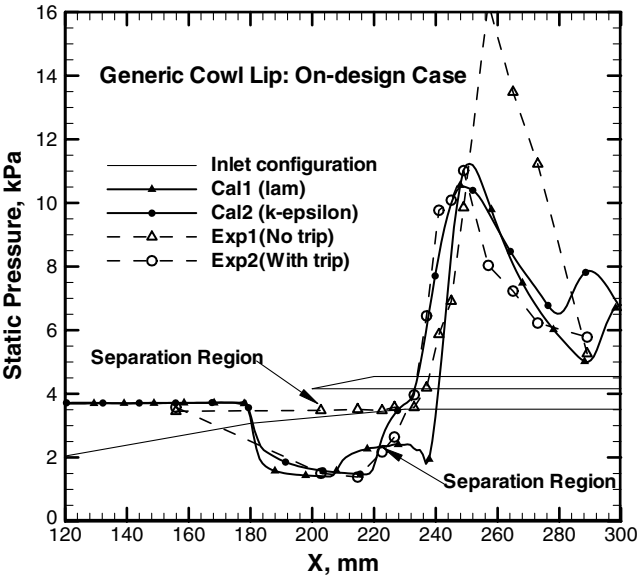

Fig. 6 Comparison of experiment and calculation results (100% cowl).

Based on the considerations mentioned above, an inlet model and its trip device were designed and tested in the wind tunnel. To compare the effect in reducing separation between the swept cowl lip and the transition, a swept cowl lip was also designed and tested.

Model Description

Flowfield structure of a general mixed-compression inlet [10] is shown in Fig. 1a. To obtain a uniform flow captured by the inlet, the cowl oblique shock is designed to impinge and vanish at the expansion corner (the junction of the inlet and the isolator). However, the oblique shock cannot impinge at the corner exactly in most designs or at an off-design condition (i.e. when the freestream Mach number is below the designed value), so the flow structure at the throat is always complicated (Fig. 1b). A tradeoff design is shown in Fig. 1c, in which the expansion corner is replaced by a continuous expansion surface at the throat.

To reduce the total pressure losing of the hypersonic flow by the oblique shocks, multistage or isentropic compressing is usually adopted in the wedge/cone and the cowl design. However, some problems will be caused by the multistage or isentropic design, such as a longer forebody and smaller first wedge/cone angle causing more friction losing and more structure weight. So, various factors must be considered in the inlet designing procedure.

The main purpose of the experiment is not to design a perfect inlet, but to study inlet performance with different boundary-layer states (laminar or turbulence). To simplify the inlet design and to reduce the machining difficulty, a "single-stage" compressing center cone (the half-cone angle is 15 deg) was used in the model, and a "two-stage" expansion instead of a single expansion corner or continuous expansion surface was applied at the inlet throat. Moreover, two kinds of the cowl lips (called generic cowl lip and swept cowl lip) were designed to test the different influence caused by the lip shape. The experimental model is shown in Fig. 2.

Mounting a boundary-layer trip device on the experimental model has been proved to be a useful forced transition method in some ground tests [11–15]. Up-to-date research about forced boundary-layer transitions of the hypersonic vehicle is mainly fastened in the NASA Langley Research Center [11–13] and Purdue University [14,15]. Detailed experimental data have also been published in their reports. A boundary-layer trip device similar to the design in [12] is adopted and shown in Fig. 3. The trip cell shape is a diamond, with a diagonal length of 2.1 mm, space between each cell of 3.6 mm, and height of 1 mm. Altogether 60 cells are equably mounted around the trip ring. Research of [12] indicates that the diamond trip cell is rather useful for the boundary-layer transition, although it greatly influences the flowfield.

By adjusting the cowl position backward or forward, the inlet CR_{in} decreases or increases. When the cowl lip is at the on-design position, the forebody oblique shock impinges on the cowl lip, and the inlet mass capture ratio is almost 100%. The distance between the cowl lip and the inlet throat L_{cowl} is defined as the reference length. "100% cowl" denotes the on-design cowl lip position, and "0% cowl" means that the cowl lip is settled at the inlet shoulder. Contractive ratios CR_{in} are 1.35, 1.23, 1.12, and 1.0 varied from different cowl lip positions of 100, 67, 33, and 0%.

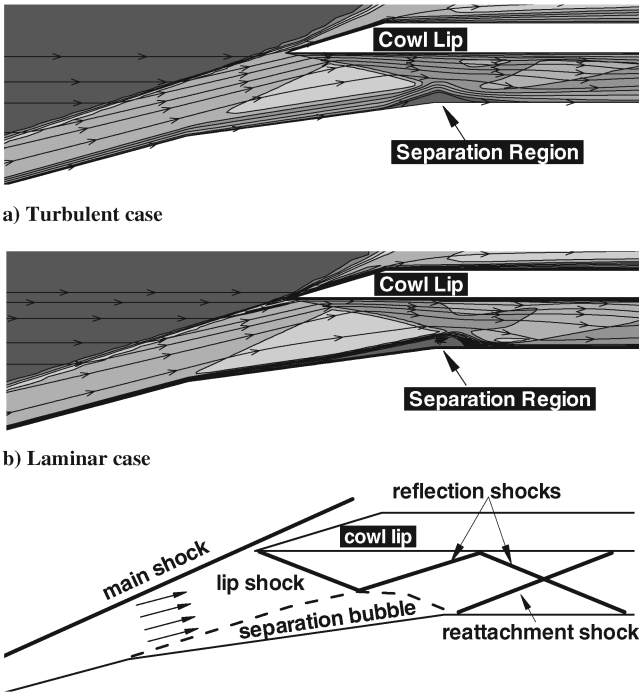

Fig. 7 Mach contours and stream lines (On-design).

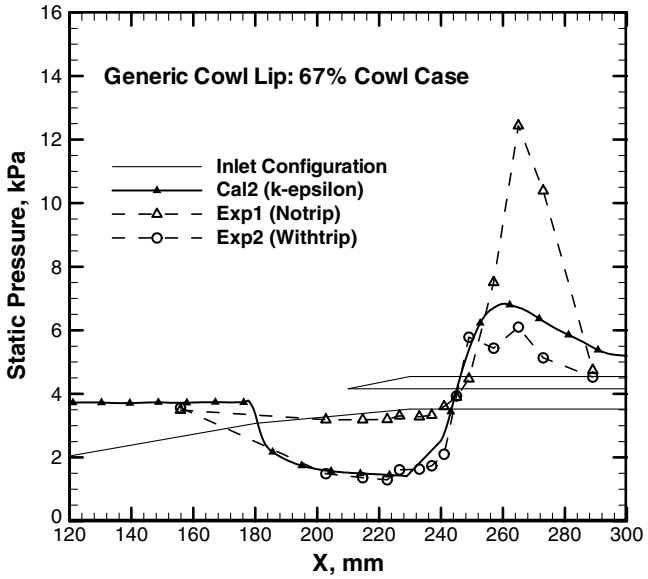

Fig. 8 Comparison of experiment and calculation results (67% cowl).

The experiment model was made of aluminum. For operation convenience, the cowl lip and the transition trip were designed as replaceable components.

Experimental Test Facility

Tests were carried out in the KD-01 gun tunnel, a typical impulsive tunnel similar to that described in [16]. The contoured, axisymmetric nozzle diameter is 500 mm. At the nozzle exit, the Mach number is 8.09, the total pressure is 4.77 MPa, the total temperature is 765 K, and the unit Reynolds number is 9.55×10^6 m^{-1}. To ensure the model was placed in a uniform flowfield and to get rid of the disturbance caused by the nozzle, the inlet model was designed relatively small. Since almost all experiences about transition indicate that the turbulent boundary layer would not occur if the Reynolds number is below 10^7 at Mach 8 [17], the natural boundary-layer transition on the inlet center cone would not take place in our experiments.

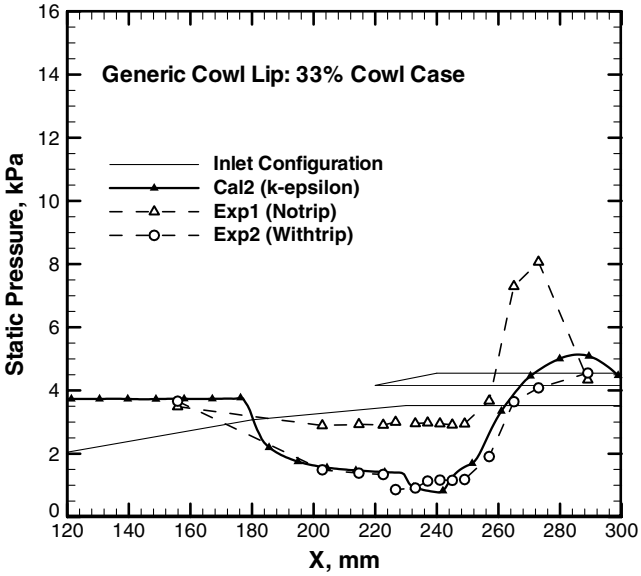

Fig. 9 Comparison of experiment and calculation results (33% cowl).

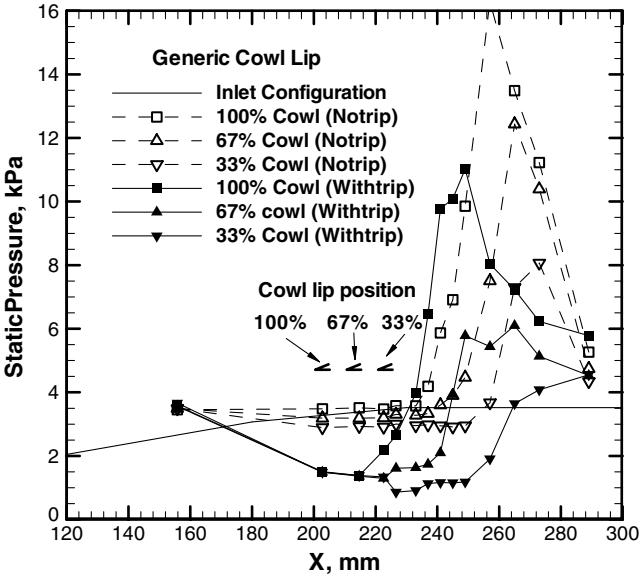

Fig. 10 Comparison of pressure distributions in different cowl positions.

The KD-01 gun tunnel and the experiment model are shown in Fig. 4. To meet the need of transient data acquiring, the transducer was directly mounted in the model, without using a long pipe to connect the orifice and transducer. A typical run result of the wind tunnel is displayed in Fig. 5, in which the vertical axis denotes the total pressure signal of the test flow. It can be concluded from Fig. 5 that the total pressure can last about 20 ms. The pressure test data of the model is the average value of the stable region. Digital schlieren photographs are acquired with a high speed CCD digital camera which is connected to the schlieren facility.

Numerical Simulation Method

The numerical results of the inlet flowfield were obtained by solving RANS (Reynolds-averaged Navier–Stokes) equations, which are closed by the k–ϵ turbulence model, and discretized by FVM (finite volume method) based on multiblock structured mesh. To calculate the turbulent flow near the wall more efficiently, a wall function is used in the turbulence model. A second-order accurate

TVD (total variable diminishing) scheme with an Osher–Chakravarthy limiter [18] is used to guarantee the shock captured accurately. The mesh number of the calculation region is about 46,000, and the first Δy of the mesh near the wall is set at only 0.02 mm to solve the boundary layer correctly.

Results and Analysis

By replacing the cowl lip or the boundary-layer trip device, several experimental items including different CR_{in} and a turbulence/laminar boundary layer were finished in the wind tunnel. Pressures along with the centerbody of the inlet were acquired from experiment data and numerical simulation results; schlieren images were acquired by a high speed CCD digital camera.

Generic Cowl Lip Cases

Experimental and calculational results of the on-design cases are shown in Fig. 6, which involve laminar and turbulence boundary-layer cases. The calculated flowfields are also shown in Figs. 7a and 7b. From these results, it can be seen that a relatively large separation region is formed near the incidence point of lip shock when the boundary layer is laminar; the separation region is relatively small if the boundary layer is turbulent. In Fig. 6, the turbulent computational data agree well with the experimental results when the trip device is used. However, the laminar calculation data cannot meet the experimental results so well at the separation region if no trip acts on the boundary layer. Based on the laminar experiment pressure data, a suppositional laminar flow structure of the inlet is exhibited in Fig. 7c. The speculating procedure about the flow structure is 1) no separation exists near the first pressure orifice, because the results of the experiment and calculation are almost coherent; 2) a separation region exists near the second to the fourth pressure orifice, because the pressure values are all close to the value of the first orifice; (3) the reattachment shock position is near the fifth or the sixth pressure orifice, because the pressures tested go up to a relatively high value.

Experimental and calculational results of the off-design cases (67% cowl and 33% cowl) are shown in Figs. 8 and 9, respectively. The pressure test data in these two cases validate the conclusion drawn from the analysis of the on-design cases, namely, a large separation region existed in the entrance of the inlet when the boundary layer swallowed by the inlet is laminar, and the boundary-layer transition could obviously reduce the separation region. In addition, the calculational results with a turbulent freestream agree well with the experimental data (with trip).

To explain the problem directly, pressure distributions acquired in the tests with different cowl positions are shown in Fig. 10. The results show that the reflected shock of the cowl lip moves backward when the cowl lip moves backward both in the laminar cases and in the turbulence cases. Also, it is clear that pressures in the separation region become smaller when the cowl lip moves backward in the laminar cases. However, even if in 33% cowl cases, the pressure value near the separation region in the laminar boundary-layer condition is about 2.1 times that in turbulence cases. We can conclude that the separation region is relatively large in the laminar cases.

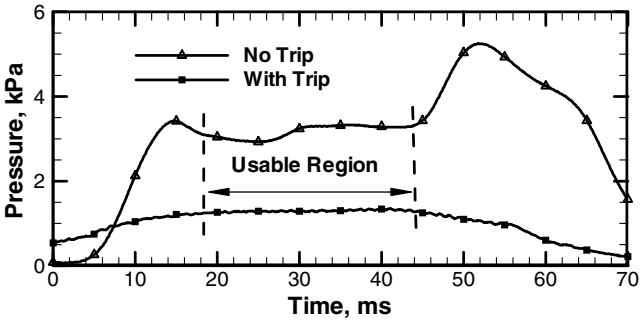

Fig. 11 Transient signal of the third pressure port in turbulent and laminar cases.

The signals of the third pressure port (near the separation region) are shown in Fig. 11. The region between the two dashed lines is the usable test time zone described in Fig. 5. Clearly, the test pressure is unstable even though the gun tunnel is in a stable state if the boundary layer stays laminar; however, the test pressure stays considerably stable if the boundary layer is transited to turbulence.

From the results and analysis mentioned above, we can draw the conclusion that the boundary trip device is successfully designed and the numerical simulation of the inlet turbulent flowfield is creditable because the experimental data agree well with the simulation results. Nevertheless, the separation region is not predicted exactly with the CFD method when the flowfield is laminar. Obviously, the laminar results stand in notable contrast against the turbulent results. Maybe this phenomenon can be attributed to the following two reasons.

1) The lip shock impinging on the center cone induces a relatively large region separation, but the numerical simulation method cannot accurately predict the flowfield with a large separation region in it. When the boundary layer is forced to be transited to turbulence, the separation region becomes smaller because the turbulent boundary layer can withstand a larger reverse pressure gradation; therefore, the numerical method can predict the flowfield and pressure distributions exactly.

2) The turbulence intensity of the wind tunnel and the roughness of the inlet model in experiment are not considered in the CFD simulation presently. So, a distinction between the laminar CFD simulation and experiment without trip may cause the difference mentioned previously.

Swept Cowl Lip Cases

The reflected oblique shock generated by the swept lip is also swept, therefore the separation possibility may be reduced, and then a better starting performance could be realized by using the swept cowl lip. To compare the efficiency of reducing separation with the transition way, experiments about the swept cowl lip were also

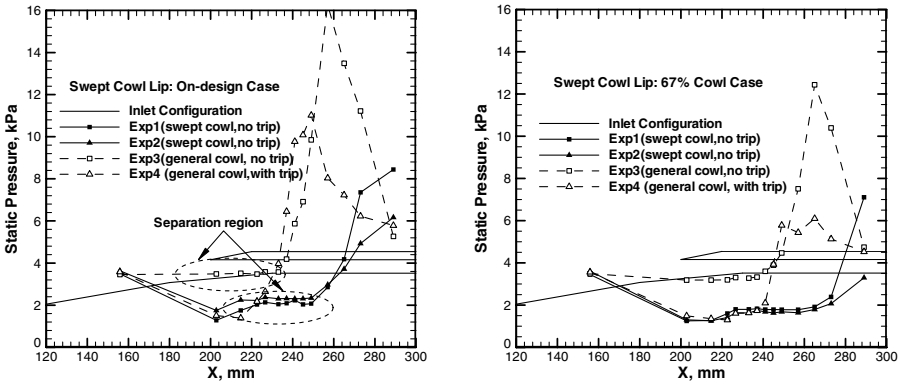

a) 100% cowl **b) 67% cowl**

Fig. 12 Experimental pressure distributions in swept cases.

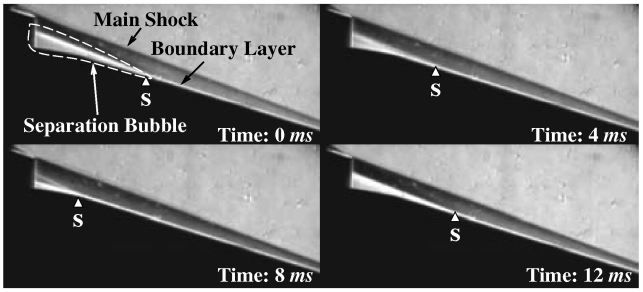

Fig. 13 Generic cowl lip, and no trip cases.

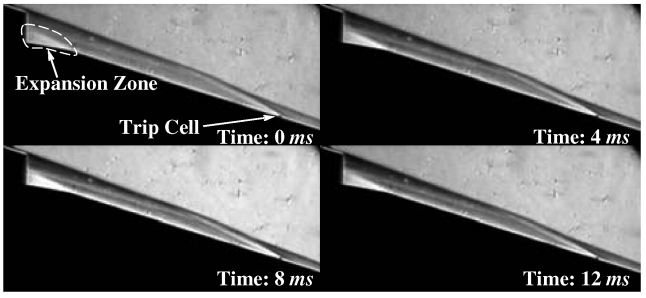

Fig. 14 Generic cowl lip, with trip cases.

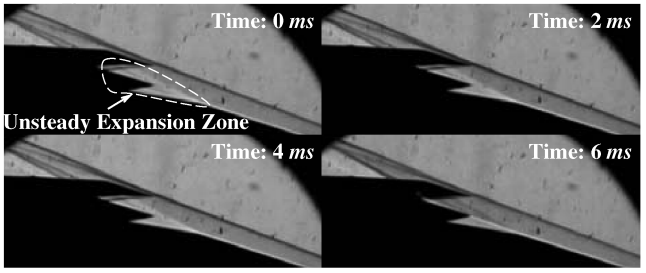

Fig. 15 Swept cowl lip, and no trip cases.

carried out in this paper.

The pressure distributions along the generatrix of the inlet center cone are shown in Fig. 12 (on-design and off-design cases). Two runs are repeated to acquire the pressure data on the two typical generatrixs shown in Fig. 2 ("Exp1" and "Exp2" shown in Fig. 12 indicate line A and line B shown in Fig. 2, respectively). As a reference, the corresponding laminar experimental results ("Exp3") and the turbulent experimental results ("Exp4") of the generic cowl lip cases are also shown in the figure. For the on-design cases, comparison of the results in the laminar state (Exp1, Exp2, and Exp3 in Fig. 12a) indicate that the separation region near the entrance of the inlet becomes smaller, for the pressures at the inlet entrance fall to a relatively low degree. However, comparison between the no tripped swept cowl lip cases and the tripped generic cowl lip cases (Exp1, Exp2, and Exp4 in Fig. 12a) indicate that a relatively large separation region still existed at the entrance of the inlet. For the off-design cases, as shown in Fig. 12b, the separation region cannot be recognized clearly by pressure distributions.

Schlieren Results

Schlieren images captured by the high speed digital camera were saved simultaneously with the pressure data during the wind tunnel runs, some of which are shown in Figs. 13–15. In these images, the forebody shock and the forebody boundary layer can be distinguished clearly. Figure 13 shows the results of the cases of the inlet mounting generic cowl lip, without a trip device. The symbol "S" denotes the separation point of the forebody boundary layer. We can see from Fig. 13 that the separation point S is not at the same location for the four different moments, and a separation bubble exists near the entrance of the inlet. Figure 14 presents the flow structure of the forced boundary-layer transition cases. Being different from Fig. 13, we can hardly observe a diversity of the flowfield from the four images, which are acquired at different moments. Comparison of Figs. 13 and 14 indicates that the trip device does transit the laminar boundary layer to turbulence, and the separation zone disappears (or cannot be observed, at least) in the transition cases (Fig. 14). Figure 15 displays the schilieren images of the swept cowl lip and no trip cases. Compared with Fig. 13, no obvious separation bubble can be observed in Fig. 15. However, an unsteady region located at the expansion zone can be found compared with Fig. 14. So, we can draw a conclusion that the cowl shock strength and separation induced by cowl shock can be reduced to some extent by the mounting swept cowl lip, but the reduction is not so distinct as using a forced boundary-layer transition.

Conclusions

Experimental results prove that the trip device is designed successfully, and the laminar boundary layer can be transited to turbulence in the hypersonic wind tunnel. The flow structure and the pressure distributions of the inlet are greatly influenced by the boundary-layer states (laminar or turbulence). That is, a relatively large separation bubble exists in laminar cases, but it can be reduced by tripping the boundary layer to turbulence.

A large separation bubble existing in the inlet can affect the pressure recovery performance and the starting performance of the inlet. Therefore, it is important to examine the boundary-layer states when the test program is planned. Also, it should be seriously considered whether the boundary layer of the inlet is turbulence or not before the experimental data are analyzed or adopted.

Application of the swept cowl lip is an efficient method to reduce separation, whereas less effective than that of the boundary-layer transition. A more detailed study about forced boundary-layer transition should be performed in future investigation.

References

[1] Van Wie, D.M., "Scramjet Inlets," *Scramjet Propulsion*, edited by E. T. Curran and S. N. B. Murthy, Vol. 198, Progress in Astronautics and Aeronautics, AIAA, New York, 2001, pp. 447–511.

[2] McClinton, C. R., Voland, R. T., Holland, S. D., and Engelund, W. C., "Wind Tunnel Testing, Flight Scaling and Flight Validation with Hyper-X," AIAA Paper 98-2866, June 1998.

[3] Holland, S. D., "Experimental Investigation of Generic Three-Dimensional Sidewall-Compression Scramjet Inlets at Mach 6 in Tetrafluoromethane," NASA TM-4479, Dec. 1993.

[4] Smart, M. K., and Trexler, C. A., "Mach 4 Performance of a Fixed-Geometry Hypersonic Inlet with Rectangular-to-Elliptical Shape Transition," AIAA Paper 2003-0012, Jan. 2003.

[5] Van Wie, D. M., Kwok, F. T., and Walsh, R. F., "Starting Characteristics of Supersonic Inlets," AIAA Paper 96-2914, July 1996.

[6] Korte, J. J., Singh, D. J., Kumar, A., and Auslender, A. H., "Numerical Study of the Performance of Swept, Curved Compression Surface Scramjet Inlets," AIAA Paper 93-1837, June 1993.

[7] Andrews, E. H., "Scramjet Development and Testing in the United States," AIAA Paper 2001-1927, April 2001.

[8] Kouichiro, T., Takeshi, K., and Daisuke, A., "A Geometrical Approach for Controlling Pressure Distributions in Scramjet Inlet and Isolator," AIAA Paper 2000-0620, Jan. 2000.

[9] Schulte, D., Henckels, A., and Neubacher, R., "Manipulation of Shock/Boundary-Layer Interactions in Hypersonic Inlets," *Journal of Propulsion and Power*, Vol. 17, No. 3, 2001, pp. 585–590.

[10] Reinartz, B. U., Herrmann, C. D., and Ballmann, J., "Analysis Of Hypersonic Inlet Flows with Internal Compression," AIAA Paper 2002-5230, Oct. 2002.

[11] Berry, S. A., Auslender, A. H., and Dilley, A. D., "Hypersonic Boundary-Layer Trip Development for Hyper-X," AIAA Paper 2000-4012, Aug. 2000.

[12] Berry, S. A., DiFulvio, M., and Kowalkowski, M. K. "Forced Boundary-Layer Transition on X-43 (Hyper-X) in NASA LaRC 20-Inch Mach 6 Air Tunnel," NASA TM-210316, Aug. 2000.

[13] Berry, S. A., DiFulvio, M., and Kowalkowski, M. K. "Forced

Boundary-Layer Transition on X-43 (Hyper-X) in NASA LaRC 31-Inch Mach 10 Air Tunnel," NASA TM-210315, Aug. 2000.

[14] Takeshi, I., Randall, L. A., and Schneider, S. P., "Effect of Free Stream Noise on Roughness-Induced Boundary-Layer Transition for a Scramjet Inlet," AIAA Paper 2000-0284, Jan. 2000.

[15] Schneider, S. P., "Hypersonic Laminar-Turbulent Transition on Circular Cones and Scramjet Forebodies," *Progress in Aerospace Sciences*, Vol. 40, Nos. 1–2, 2004, pp. 1–50.

[16] Sullivan, P. A., Deschambault, R. L., Hawboldt, R. J., and Gordon, K. A., "Tunnel Development, Operation and Calibration," *Investigation in the Fluid Dynamics of Scramjet Inlets*, Ryerson Polytechnical Univ. and Univ. of Toronto, Toronto, July 1992.

[17] Heiser, W. H., and Pratt, D. T., "*Hypersonic Airbreathing Propulsion*," AIAA Education Series, AIAA, New York, 1994, p. 43.

[18] Chakravarthy S. R., "High Resolution Formulations for the NS Equations," N89-17824, 1989.